

A Real-Time Active Vibration Controller

M.R. Serbyn

W.B. Penzes

Center for Manufacturing
Engineering, National
Bureau of Standards

The Michelson interferometer is viewed as a noisy system whose noise input results from unwanted changes in the optical path lengths of its beams, and whose desired output is a constant optical path-length difference. A technique for maintaining this quality at a value equal to a multiple of quarter wavelengths of the light is described.

INTRODUCTION

Most applications of the Michelson interferometer (Figure 1) to metrology are based on effecting a change in the optical path-length difference by means of the parameter whose value is to be measured. Because the optical path lengths of the interfering beams may also be sensitive to other mechanical, acoustic, or thermal disturbances, the system must be considered as inherently noisy. Passive methods to control this noise can be very successful, but one finds many situations where they are not practicable. Although the active approach has been used for stabilizing the frequency of gas lasers^(1,2) and also for stabilizing the optical paths of interferometers,^(3,4) the design philosophy underlying the system here described is unique. Control of the optical path-length difference is accomplished by periodically comparing the phase difference between the fundamental and the second-harmonic components of the photodetector output. Using this information, a logic unit causes positive- or negative-going ramp signals to be generated in the feedback loop and applied to the "fixed" mirror as a path-length correction.

Presented at the Vibration Instrumentation and Control session of the 27th International Instrumentation Symposium, 1981, Indianapolis. Government authors; no copyright claimed.

THEORETICAL BASIS

Harmonic analysis of the output of a phase-modulated interferometer results in the following well-known expression of the photodetector current:⁽⁵⁾

$$i = A + B \left(\cos \frac{4\pi}{\lambda} \Delta \right) \cdot \left\{ J_0 \left(\frac{4\pi}{\lambda} d \right) - 2J_2 \left(\frac{4\pi}{\lambda} d \right) \cos 2\omega t + \dots \right\} \\ - B \left(\sin \frac{4\pi}{\lambda} \Delta \right) \cdot \left\{ 2J_1 \left(\frac{4\pi}{\lambda} d \right) \cos \omega t - 2J_3 \left(\frac{4\pi}{\lambda} d \right) \cos 3\omega t + \dots \right\} \quad (1)$$

where

$\Delta = L_1 - L_2$ (see Figure 1)

A and $B =$ constants

$d, \omega =$ the amplitude and angular frequency, respectively, of the displacement $d \cos \omega t$ that is being measured

$\lambda =$ the wavelength of the light source

$t =$ time

The quantities $J_p(x)$ are Bessel functions of the first kind of order p .

For most methods of processing the photodetected signal, it is either necessary or convenient to fix the unmodulated path-length difference 2Δ . The usual requirement is that $\Delta = (2n+1) \lambda/8$, $n=0,1,2,\dots$, which effectively

eliminates from the output all even harmonics and maximizes the odd ones. The device labeled "Stabilizer" in Figure 1 performs this function automatically. Before explaining its operation it is important to show how continuous changes in Δ are transformed into discrete changes in phase.

The first- and second-harmonic terms in Equation 1 can be rewritten as:

$$i_1 = -B \cdot J_1 \left(\frac{4\pi}{\lambda} d \right) \cdot \left[\cos \left(\omega t + z - \frac{\pi}{2} \right) + \cos \left(\omega t - z + \frac{\pi}{2} \right) \right]$$

and

$$i_2 = -B \cdot J_2 \left(\frac{4\pi}{\lambda} d \right) \cdot \left[\cos(2\omega t + z) + \cos(2\omega t - z) \right] \quad (2)$$

$$\text{where } z = \frac{4\pi}{\lambda} \Delta$$

At a given value of the displacement d (commonly, $d < \lambda/2$) and with a constant Δ , the phase ϕ of $i_2(t)$ relative to $i_1(t)$ is the same at times one vibration period apart. If Δ is perturbed, ϕ can either change by 180° or not change at all, depending on the amount of perturbation. This result follows from Equation 2. It can be obtained either algebraically or, more simply, by means of phasor diagrams. Choosing the latter approach, consider two examples, one vibration cycle apart, under changing path-length conditions such that $0 < \Delta < \frac{\lambda}{8}$ when $\omega t = 0$ and $\frac{\lambda}{8} < \Delta < \frac{\lambda}{4}$ when $\omega t = 2\pi$.

Figure 2a shows the corresponding phase relationships of the first and second harmonics. The noteworthy feature of these diagrams is that the instantaneous phase difference between the first and second harmonics is either 0 or π regardless of the magnitude of Δ . This property is also true for all other adjacent quadrants of $\frac{4\pi}{\lambda} \Delta$.

The degenerate case of $\frac{4\pi}{\lambda} = n \frac{\pi}{2}$ where $n = 0, 1, 2, 3, \dots$ corresponds to the desired $\Delta = n \frac{\lambda}{8}$.

If the phases of the two harmonics are shifted, as for example, by tracking filters,

$$\pi = \omega t - \theta + \epsilon \pi \quad (3)$$

where θ is relative phase shift introduced by signal conditioning, and $\epsilon \pi$ is the randomly occurring change in phase produced by a disturbance of the quiescent value of Δ .

$$\begin{aligned} \epsilon &= 0 \text{ for } 2n \frac{\lambda}{8} < \Delta < (2n + 1) \frac{\lambda}{8} \\ &= 1 \text{ for } (2n - 1) \frac{\lambda}{8} < \Delta < 2n \frac{\lambda}{8} \\ &= \frac{1}{2} \text{ for } \Delta = n \frac{\lambda}{8}, n = 0, \pm 1, \pm 2, \dots \end{aligned} \quad (4)$$

Figure 2B shows a plot of ϵ as a function of Δ .

The control strategy now becomes evident: monitor the phase difference ϕ and generate a signal to correct the deviation from $\Delta = (2n + 1) \lambda/8$.

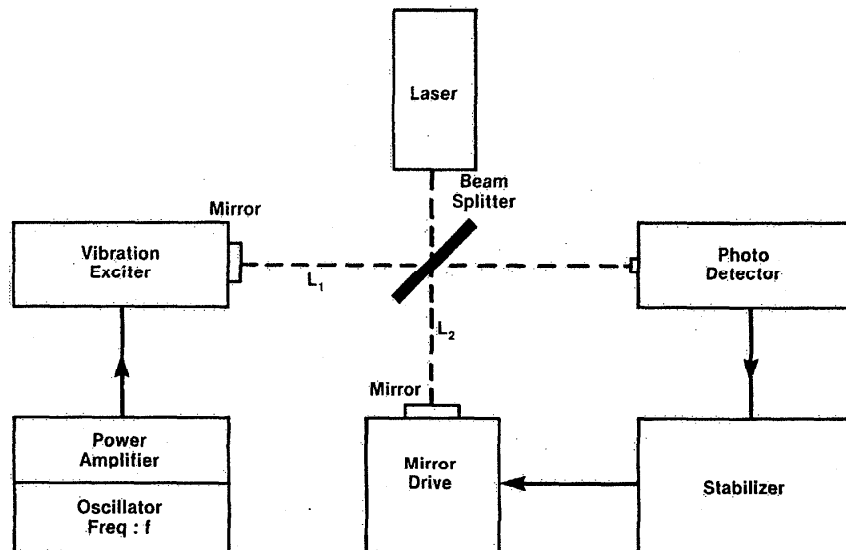


Figure 1. An interferometer system retrofitted with the stabilizer

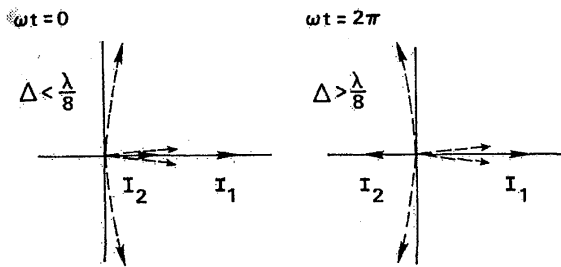


Figure 2A. Phasor diagrams representing two successive samples of the fundamental (I_1) and second-harmonic (I_2) components of the photodetector current

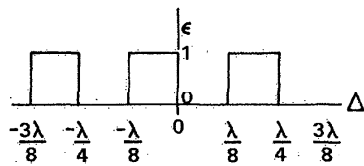


Figure 2B. Dependence of the randomly occurring number on Δ

OPERATIONAL DESCRIPTION

Figure 3 shows the functional components of the control system. The signal conditioner filters the output of the photodetector to select the fundamental and second-harmonic components and converts them to precise square waves. The phase comparator, which accepts

these square waves, functions as an AND gate. Its output can be in one of three states:

- (1) When the amplitude of the fundamental component is maximized (the second-harmonic amplitude is approximately zero), the zero output of the phase comparator sensed by the null detector causes the track-and-hold amplifier to hold the correcting-voltage level of the ramp generator and output amplifier constant as long as the path-length difference remains constant.
- (2) When $-\pi < \phi < 0$, the output of the phase comparator is one positive pulse for each cycle of the fundamental.
- (3) When $0 < \phi < \pi$, the output of the phase comparator consists of two positive pulses for each cycle of the fundamental.

The pulses representing states 2 and 3 are counted by two counters. One of the counters gets a reset pulse after each cycle of the fundamental component, while the other is reset only when the phase comparator is in state 3. The outputs of the counters are decoded and used to trigger a bistable switch. Its outputs are in turn "AND-ed" with the outputs of the null detector and the limit detector for the purpose of turning on and off the positive or negative charging voltages of the ramp generator, as required by the condition of the phase comparator, after amplification, is applied to a PZT cylinder serving as a mirror drive to correct the deviations from the desired value of the optical path-length difference. The track-and-hold amplifier output

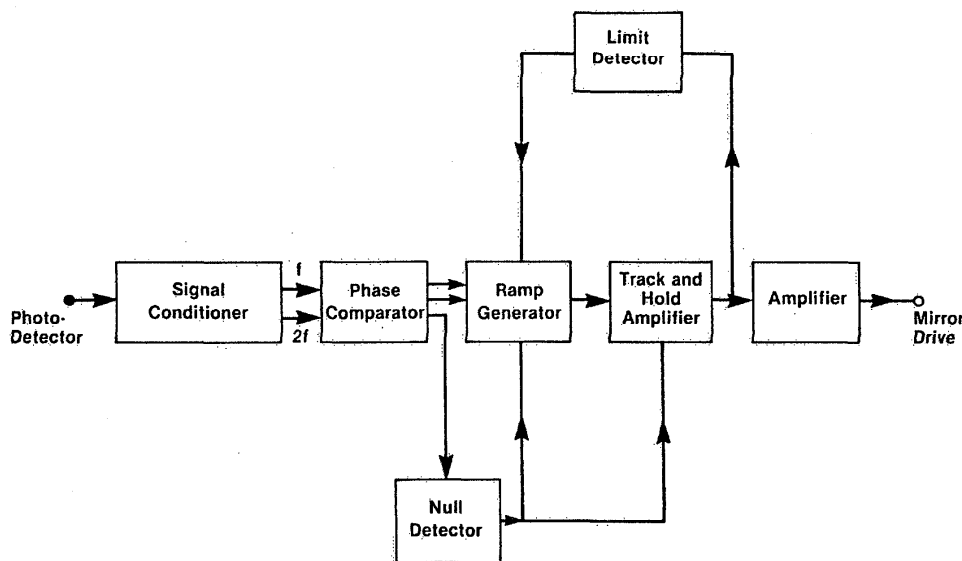


Figure 3. Optical path-length-difference stabilizer (functional diagram)

also controls the limit detector, which resets the charging voltage to approximately zero in order to keep the amplifier output within predetermined limits. This ensures that the device locks on the nearest fringe.

PERFORMANCE EVALUATION

Prior to complete system evaluation, the response of the phase comparator alone was carefully examined under both controlled and real-life conditions. Figure 4 presents a set of typical results at 12.5 kHz as the fundamental frequency. The phase ϕ of $\sin(2\omega t + \phi)$ referenced to $\sin \omega t$ was varied from 0 to 2π and locked at each of the steps shown. With those signals as input, the output of the phase comparator consisted of one or two pulses per vibration cycle, as required by the design. In the light of the results of Figure 4, the optimum value of ϕ in Equation 3 appears to be $\pm 90^\circ$. A variable phase shifter was, therefore, added to the signal conditioner unit of Figure 3.

INPUT

$$i_1 = \sin \omega t$$

$$i_2 = \sin(2\omega t + \phi)$$

$$\phi = 0^\circ$$

OUTPUT

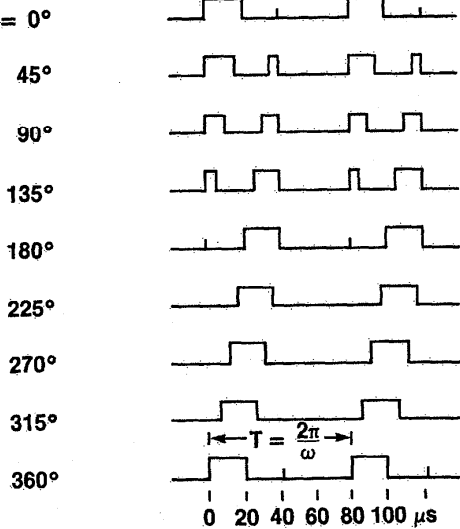


Figure 4. Phase comparator response at 12.5 kHz

Two tests of performance were used to qualify the stabilizer. The first consisted of comparing time histories of the photodetector output with and without stabilizer. The rms value of the fundamental component was monitored. Figure 5 shows two typical samples obtained under deliberately noisy conditions. With the stabilizer operative, the change in the level of this quantity is seen not to exceed 0.1 dB. The other performance test was carried

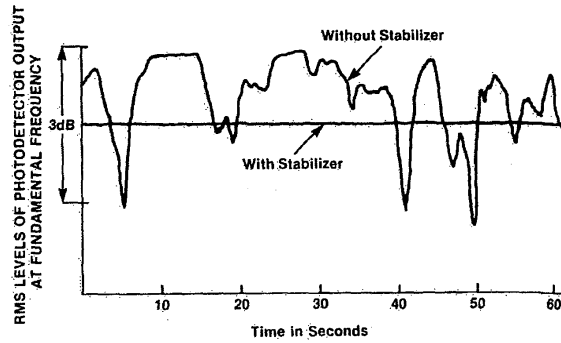


Figure 5. RMS levels of photodetector output at the fundamental frequency

out in the frequency domain. A real-time spectrum analyzer was used to observe the with/without conditions and to compare the power-spectral densities of the fundamental and second-harmonic components of the photodetector output. The second-harmonic level was typically between 40 and 45 dB below that of the first-harmonic level. The apparent inability to increase this difference was subsequently traced to the presence of about 1 percent second-harmonic distortion in the vibration exciter used for the tests.

MATHEMATICAL MODELING

To assess more generally the potential of the concept for active vibration control, a computer simulation of the control loop was executed. The parameters of the mathematical model included the sampling rate, the corrective-ramp slope, time delays, and input-noise characteristics. To highlight the corrective action and to keep the model simple, the controlled variable, feedback signal, and reference signal were all expressed in terms of the optical-path-length difference. Figure 6 shows the structure of this model and the relationship between its parameters. The actual value of the optical path-length

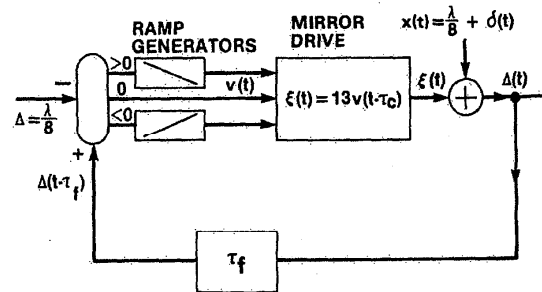


Figure 6. Simplified mathematical model of the stabilizer considered as a noise control device

ifference $\Delta(t)$ is continually compared with the desired constant value of $\lambda/8$. Based on this comparison appropriate ramp voltages $v(t)$ are developed to drive a ZT transducer having a sensitivity of 13 nm per volt. The corrective displacement signal $\xi(t)$ is then added to the noisy input. The model was found to be quite insensitive to realistic changes in the values of the time delays τ_i and τ_c .

A typical noise environment $\delta(t)$ of the interferometer used in this research was found to contain several line components and a continuous spectrum. Figure 6 shows the results of a simulation with this type of disturbance added to the desired value of Δ . The input is considered to be $\lambda/8 + \delta(t)$, the output is $\Delta(t)$. (The spectra appearing in Figure 7(a) are Fourier transforms of these signals.) The correction signal is to be identified with $\xi(t)$ of Figure 6. Both the time- and frequency-domain representations are used to test the effectiveness of the corrective action.

CONCLUSIONS

On the basis of experimental tests and mathematical simulation, it can be concluded that the active method of noise control fully satisfies the requirements of the prob-

lem addressed in this paper. Moreover, the results of the investigation here reported indicate a more general applicability of the concept. To demonstrate this, a noise control system independent of the interferometer has been constructed and will be reported in a subsequent paper. It must, however, be emphasized that some knowledge of the noise characteristics is required for choosing optimum values of the design parameters.

REFERENCES

1. Shimoda, K. and Javan, A., 1965. Stabilization of the He-Ne maser on the atomic line center. *J. Appl. Phys.* 36 (3); 718 (March 1965).
2. White, A.D., 1967. Control system for frequency stabilizing a 6328 Å gas laser. *Rev. Sci. Instr.* 38, (8): 10789. (August 1967).
3. Palmer, C.H. and Green, R.E., 1977. *Appl. Opt.* 16: 2333; *Mater. Eval.* 35 (10): 107.
4. Kline, R.A. and Green, R.E., 1978. A comparison of optically and piezoelectrically sensed acoustic emission signals. *J. Acoust. Soc. Am.* 64 (12): 1633.
5. Schmidt, V.A. et al., 1961. Optical calibration of vibration pickups at small amplitudes. *J. Acoust. Soc. Am.* 33 (6): 748.

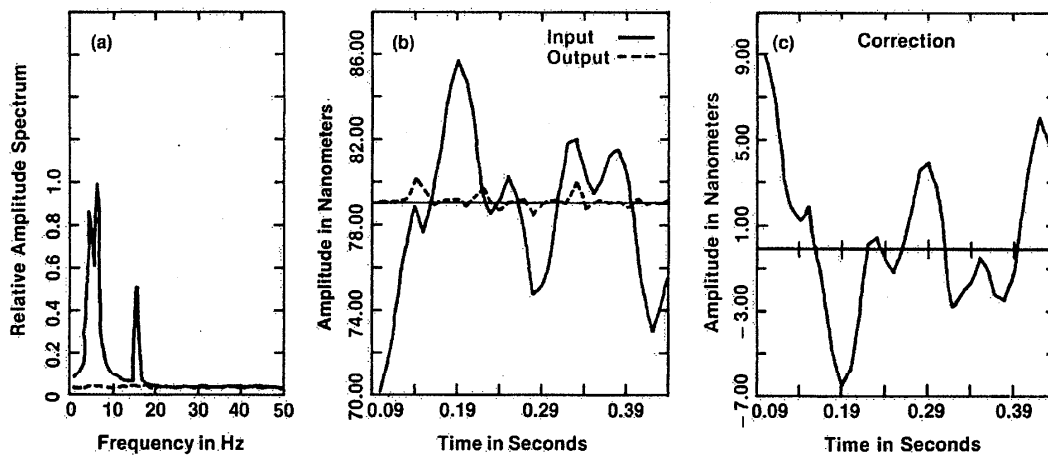


Figure 7. Control of the optical-path-length difference about $\Delta = \lambda/8 = 79.1$ nm, showing (a) input and output spectra; (b) input and output time histories; (c) control signal